Effects of lattice strain and ion displacement on the bonding mechanism of the ferroelectric perovskite material $BaTiO_3$: first-principles study

2007 J. Phys.: Condens. Matter 19 276213

(http://iopscience.iop.org/0953-8984/19/27/276213)

IOP PUBLISHING JOURNAL OF PHYSICS: CONDENSED MATTER

J. Phys.: Condens. Matter **19** (2007) 276213 (14pp) doi:10.1088/0953-8984/19/27/276213

Effects of lattice strain and ion displacement on the bonding mechanism of the ferroelectric perovskite material $BaTiO_3$: first-principles study

H B Shu[1,2], G C Zhou[1,2], X L Zhong[1,2], L Z Sun[1,2,3], J B Wang[1,2], X S Chen[3] and Y C Zhou[1,2]

[1] Key Laboratory for Low Dimensional Materials and Application Technology of Ministry of Education, Xiangtan University, Xiangtan 411105, Hunan, People's Republic of China
[2] Institute of Modern Physics, Xiangtan University, Xiangtan 411105, Hunan, People's Republic of China
[3] National Laboratory for Infrared Physics, Shanghai Institute of Technical Physics, Chinese Academy of Science, Shanghai 20083, People's Republic of China

E-mail: lzsun@xtu.edu.cn and Zhouyc@xtu.edu.cn

Received 8 November 2006, in final form 3 June 2007
Published 21 June 2007
Online at stacks.iop.org/JPhysCM/19/276213

Abstract

The effects of lattice strain and ion displacement on the bonding mechanism of the perovskite material $BaTiO_3$ have been studied by using the density-functional theory within the full-potential linear augmented plane wave (FP-LAPW) method. The valence and the bonding charge density, the density of states (DOS), the local DOS and the partial DOS were calculated to investigate the bonding mechanisms. The charge transfer, along with the bonding process, was analysed by using the atoms in molecules theory (AIM). Based on the analysis of the bonding and the topological characteristics, the evolution of the bonding strength according to different lattice strains and ion displacements along with the phase transition of $BaTiO_3$ is shown quantitatively. Moreover, the evolution of the spontaneous polarization of $BaTiO_3$ corresponding to the ion displacements is also discussed by a modern theory of polarization in the present paper.

1. Introduction

Ferroelectric perovskite materials have been drawing widespread attention in recent years for their potential applications in the domain of microelectronics and the photoelectron industry [1, 2]. Within this family of materials, most of them have the chemical formula ABO_3, where A is a relatively large cation sitting at the corners of the unit cell, B is a relatively small cation sitting at the centre of the unit cell, and O is the oxygen anion sitting at face-centred positions. Above the Curie temperature, most of them have ideal cubic crystal structure.

As the temperature is lowered, they transform from the high-symmetry paraelectric phase to slightly distorted ferroelectric structures with tetragonal, orthorhombic and rhombohedral symmetries. Typically, the phase transitions are characterized by a small macroscopic lattice strain and microscopic displacement of ions [3–10]. The lattice distortions give rise to many changes of the microscopic and the macroscopic properties, such as bonding mechanism, charge distribution, electronic structure and spontaneous polarization, etc. Therefore, a large number of theoretical and experimental works have focused on the effects of lattice strain and ion displacements in the ferroelectric perovskite materials [3]. Those studies have demonstrated successfully the changes of the properties of perovskite, such as dielectric permittivity, piezoelectricity, pyroelectricity and spontaneous electrical polarization, according to the lattice strain and the ion displacements. However, there are very few studies that have focused on the evolution of the bonding mechanism of ferroelectric perovskite materials according to the lattice distortions, to our knowledge.

It is well known that the microscopic bonding characteristics of materials determine their macroscopic properties [11]. In particular, the bonding mechanism is one of the most important issues to reveal the origin of ferroelectric instability and ferroelectric distortion. For example, Cohen [12] has pointed out that the strong hybridization between the Ti 3d states and the O 2p states contributes to forming a strong covalent bond, which is essential for the ferroelectric instability of the perovskite oxides $ATiO_3$ (A = Ba, Pb). Therefore, the bonding mechanism is one of the aspects of most concern in the research of the materials. Previous works [12–15] have shown the relationship between the bonding mechanism and the origin of ferroelectric instability. For example, the strong p–d hybridization causes a large amount of valence charge to return to Ti in the TiO_3 unit, which makes the static charge of Ti significantly less than +4 and the static charge of O more or less neutral, rather than having a charge of −2 [1, 12, 13]. Although the above researches supply the understanding of materials' microscopic properties, most of them remain in a qualitative stage, to some extent. There is no doubt that quantitative analysis is preferable for the understanding of the bonding mechanism.

In the present paper, we have carried out full potential linear augmented plane wave (FP-LAPW) total energy calculations to investigate systematically the effects of lattice strain and ion displacement on the bonding mechanism of a paradigmatic perovskite oxide, $BaTiO_3$. The present paper aims at the study of the evolution of the bonding mechanism according to the lattice distortions. Technically, in order to give a quantitative description of the relationship between the bonding mechanism and lattice distortions, a topological analysis [16] following Bader's 'atoms in molecules' theory has been used. The understanding of the evolution of the bonding mechanism according to the lattice strain and the ion displacements is also expected to be applicable to other perovskite materials.

2. Computational details and method

$BaTiO_3$ shows a very rich phase diagram. Above the Curie temperature, it is a cubic perovskite crystal structure (paraelectric phase), as shown in figure 1. It undergoes three consecutive ferroelectric distortions along the directions [001] (tetragonal), [110] (orthorhombic), and [111] (rhombohedral) at 400, 280 and 185 K, respectively [17]. In the present paper, the emphasis is put on the bonding mechanisms of the cubic phase and the tetragonal phase. The calculations of the electronic structures and the bonding mechanism were performed by using the WIEN2k FP-LAPW package [18], within the framework of the density functional theory [19]. We adopted the Perdew–Burke–Ernzerhof (PBE) functional to describe the exchange–correlation interaction [20]. In order to ensure good convergence, the muffin-tin radius and the number of k-points to generate the final results were chosen carefully after optimization. A satisfactory

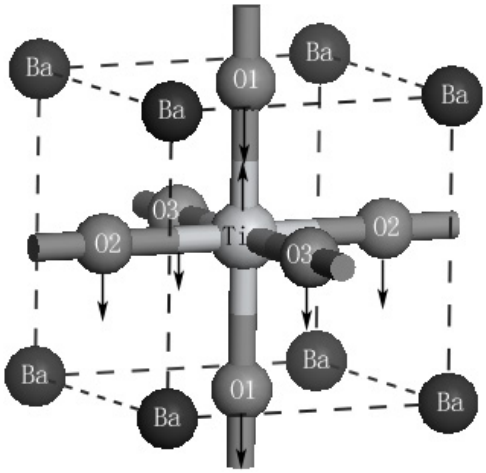

Figure 1. Ideal cubic structure of $BaTiO_3$. Internal displacement (indicated by the arrows) transforms the ideal cubic structure into the tetragonal phase.

convergence has been achieved by considering a number of FP-LAPW basis functions up to $R_{\mathrm{MT}}K_{\max} = 9.0$. R_{MT} is the muffin-tin radius and $K_{\max}$ is the maximum value of the plane wavevector that determines the so-called energy cutoff for the plane wave expansion. The self-consistent iteration was considered to converge when the total energy and the total charge in the atomic sphere were stable within 10^{-4} eV per unit cell and 10^{-4} electron charges per atom, respectively. The spin–orbit (SO) coupling is a relativistic effect which scales with the atomic number of the atoms in the materials. The perovskite materials contain the heavy elements Ba, so the effect of SO coupling was also included in the present study.

After the convergence of the self-consistent calculations, the valence charge density ρ and the bonding charge density $\Delta\rho(r)$ of the materials are obtained. The bonding charge density is defined as the difference between the total charge density in the solid and the superpositions of neutral atomic charge densities placed at atomic sites, i.e. [21],

$$\Delta\rho(r) = \rho_{\mathrm{solid}}(r) - \sum_{\alpha} \rho_{\alpha}(r - r_{\alpha}), \tag{1}$$

where $\rho_{\mathrm{solid}}(r)$ is the charge density of the crystal, and $\rho_{\alpha}(r - r_{\alpha})$ is the charge density of the atom α. The valence charge density and bonding-charge density can give a description of the charge distribution and the net charge redistribution as atoms are brought together to form a crystal, however, the description is a qualitative one. As we know, they are, to some extent, on the qualitative stage. In order to give a quantitative description of the charge transfer accompany with the bonding process, we carried out calculations based on the topological analysis [16, 22–29] following Bader's 'atoms in molecules' (AIM) theory.

The AIM theory is an useful tool to extract chemical information from the charge density [16, 27]. With such an analysis, one can go beyond a purely qualitative description of the nature and the strength of interatomic interactions. In particular, it provides a rigorous definition of the chemical bonds for all classes of molecules and solids which cover the different kinds of chemical bonds such as ionic, covalent, hydrogen bonds and other intermolecular contacts [30]. The charge density $\rho(r)$ is a scalar field defined over three-dimensional space. The topological properties of such a scalar field are conveniently summarized in terms of the number and the kind of its critical points (CPs). CPs are points where the first derivatives of $\rho(r)$ vanish, and they thus corresponding to the extreme points in the charge density—

maxima, minima, or saddles. So, the topological features of the total electron density $\rho(r)$ can be characterized by analysing its gradient vector field. Critical points are located at points r_{cp}, where $\nabla\rho(r_{cp}) = 0$, and the nature of each CP is determined from the curvatures $(h1, h2, h3)$ of the density at this point. The latter are obtained by diagonalizing the Hessian matrix of the electronic density scalar field. The Hessian matrix is

$$H_{ij} = \frac{\partial^2\rho(r)}{\partial x_i \partial y_j} \qquad (i, j = 1, 2, 3). \tag{2}$$

After diagonalization,

$$h_1 = \frac{\partial^2\rho(r)}{\partial x_1 \partial y_1} \qquad h_2 = \frac{\partial^2\rho(r)}{\partial x_2 \partial y_2} \qquad h_3 = \frac{\partial^2\rho(r)}{\partial x_3 \partial y_3}. \tag{3}$$

According to the AIM theory, each CP is denoted by a pair of integers (ω, σ), where ω is the number of non-zero eigenvalues of the Hessian matrix $H(r)$ and σ is simply the algebraic sum of the signs of the three eigenvalues. In a three-dimensional stable structure, four types of CP can be found. A CP $(3, -3)$ corresponds to local maxima of $\rho(r)$ which occur at atomic nuclear positions or at so-called non-nuclear attractors in rare cases [31]. A CP $(3, -1)$ with one positive eigenvalue is called a bond CP which corresponds to the saddle points of $\rho(r)$. Such a CP is found between every pair of neighbouring nuclei. CP $(3, +1)$ is called a ring CP, where $\rho(r)$ is minimum in the plane defined by the axes associated with the two positive curvatures and maximum in the third direction (such CPs are found within rings of bonded atoms). CP $(3, +3)$ is called a cage CP that corresponds to a local minimum of $\rho(r)$ (the cage CPs locate inside a cage nuclear arrangement). The numbers of each type of CP obey the following relationship, depending on the nature of the system:

$$N(-3) - N(-1) + N(1) - N(3) = 0, \text{ or } 1. \tag{4}$$

The number in the brackets is σ. The sum is equal to 0 or 1 for a crystal or an isolated system, respectively. The Laplacian of the electronic density $\nabla^2\rho(r)$ is given by the trace of $H(r)$. The Laplacian is positive and large for ionic bonding, but it is small or negative for covalent bonds. Within the AIM theory, a basin is associated to each attractor $(3, -3)$ CP which is defined as the region containing all gradient paths terminating at the attractor. The boundaries of this basin are never crossed by any gradient vector trajectory $\nabla\rho(\vec{r})$ and they satisfy $\nabla\rho(\vec{r}) \cdot n(\vec{r}) = 0$, where $n(\vec{r})$ is the normal to the surface at point r. The corresponding surface is called the zero-flux surface, and it defines the atomic basin when the attractor corresponds to a nucleus. Based on this space partitioning, the atomic charges deduced by integrating over the whole basin are uniquely defined. By analysing the CPs, Laplacian and the basin charge, the bonding mechanism of $BaTiO_3$ can be shown clearly and quantitatively.

In order to clearly describe the evolution of the spontaneous polarization according to the ion displacements, we calculated the spontaneous polarization based on the modern theory of polarization [32–34]. The calculations were carried out within a generalized gradient approximation (GGA) with a plane wave basis set and projector augmented wave pseudopotentials using the Vienna *ab initio* Simulation Package (VASP) [35, 36]. The plane wave energy cutoff was 400 eV. Brillouin zone integration was obtained by calculating Kohn–Sham wavefunctions for a grid equivalent to an $8 \times 8 \times 8$ Monkhorst–Pack grid for a primitive perovskite cell. Moreover, we use 10 k points along the string of polarization to obtain the electronic contribution to the polarization.

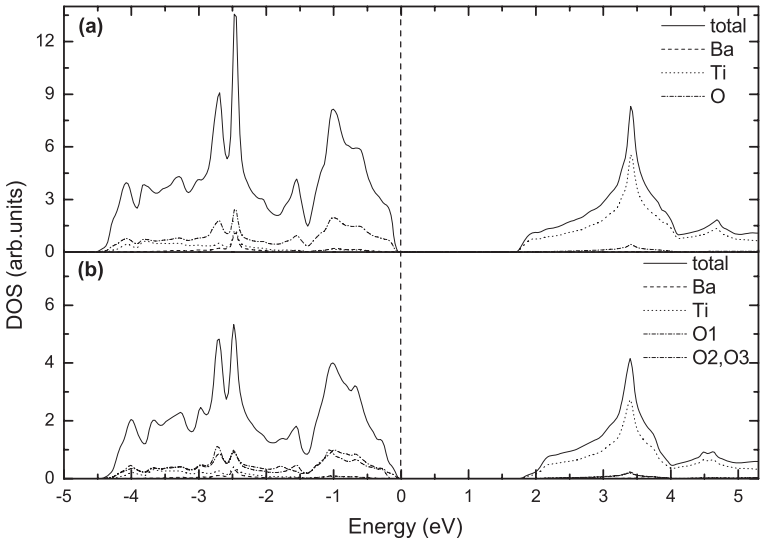

Figure 2. Calculated DOS and LDOS of $BaTiO_3$ for cubic phase (a) and tetragonal phase (b). The dashes, dotted and dashed–dotted lines denote the LDOS of Ba, Ti and O, respectively. The Fermi level is set to the zero point. The Fermi level in the following DOS figures is set in the same way.

3. Results and discussion

3.1. Bonding mechanism of equilibrium structure

The equilibrium structures of $BaTiO_3$ for the cubic phase and tetragonal phase were obtained by calculating the total energy as a function of different volumes around the experimental value. Then, the total density of state (DOS) and the local DOS (LDOS) of $BaTiO_3$ were calculated; they are shown in figure 2. The figures indicate that the valence band maximum (VBM) and the conduction band minimum (CBM) mainly come from the Ti 3d states and the O 2p states respectively for both cubic and tetragonal phase. The results not only reveal the strong coupling between the O 2p states and Ti 3d states, but also show the contribution of the Ba atom to the valence band. We make a comparison of the total DOS and LDOS between the cubic phase and the tetragonal phase by integrating the valence band (from -4.7 eV to Fermi level). For the cubic phase, the contributions of Ba, Ti, and O to the valence band are 3.4%, 10.0%, and 86.6% (O1 = O2 = O3), respectively, whereas for the tetragonal phase, the contributions of Ba, Ti, O1 and O2 plus O3 are 3.0%, 9.7%, 27.5%, and 59.8%, respectively. The results indicate that the contribution of the TiO_3 unit to the valence band in the tetragonal phase is larger than that in the cubic phase. The results also indicate that the contribution of Ti, O1, and Ba ions to the valence band decreases, whereas the contribution of O2 and O3 ions increases as the ferroelectric phase transition. The deflections mainly come from the effects of ion displacements and lattice strain, and the details will be discussed below.

The valence charge density and the bonding charge density of $BaTiO_3$ for the cubic phase and the tetragonal phase have been calculated, and they are shown in figure 3. Figures 3(a) and (c) show the calculated valence charge density for the cubic and the tetragonal $BaTiO_3$, respectively. The distribution of the charge density around the Ba ion indicates that the bonding between Ba and the TiO_3 unit is mainly ionic in nature. In the TiO_3 unit, there are some sharing charges between Ti and O, which show some covalent characteristics of the Ti–O bond. The bonding charge density is shown in figures 3(b) and (d) for the cubic phase and the tetragonal

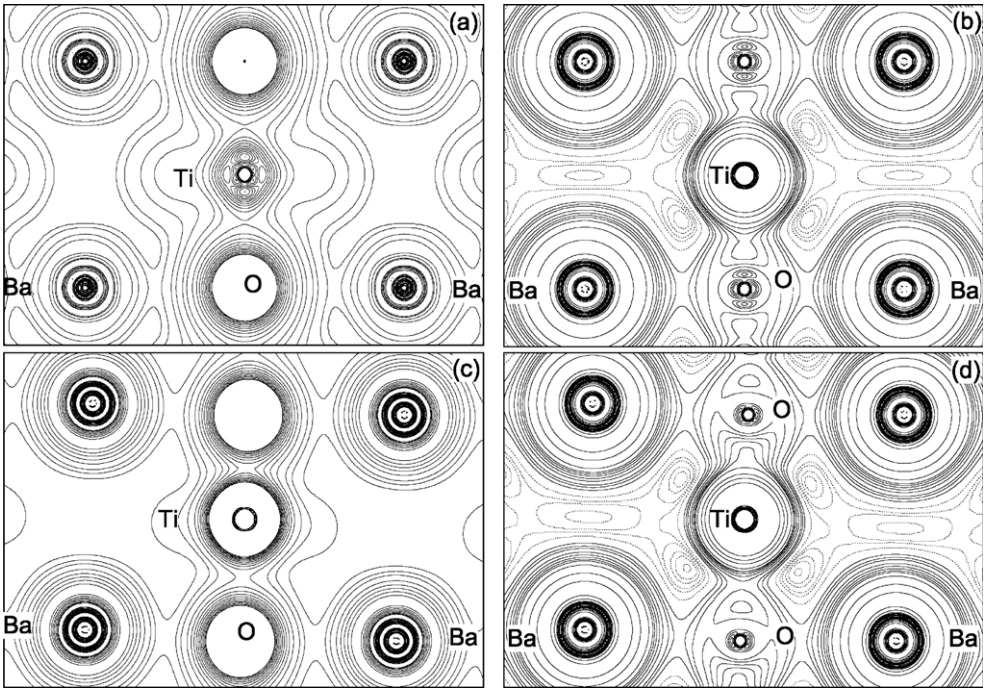

Figure 3. Valence charge density and bonding charge density of $BaTiO_3$ in the [110] plane for both cubic and tetragonal phases. (a) and (b) are the valence charge density and the bonding charge density for the cubic phase, respectively. (c) and (d) are the valence charge density and the bonding charge density for the tetragonal phase. The contour step size is 1.5×10^{-2} e/au^3 for the valence charge density and 1.8×10^{-3} e/au^3 for the bonding charge density.

Table 1. Average atomic basin charge (e^-) within the atomic basin of Ba, Ti and O calculated according to Bader's topological analysis. The negative value means charges transfer into the atomic basin and the positive value means charges transfer out of the atomic basin in the bonding process.

	Ba	Ti	O1	O2	O3	Method
Cubic phase	1.547	2.225	−1.255	−1.255	−1.255	First principles + AIM
Tetragonal phase	1.550	2.210	−1.232	−1.260	−1.260	First principles + AIM
Cubic phase	1.48	1.86	−1.29	−1.29	−1.29	Empirical model[a]
Cubic phase	1.39	1.79	−1.39	−1.39	−1.39	First principles[b]
Nominal charge	2	4	−2	−2	−2	—

[a] Reference [37].
[b] Reference [38].

phase, respectively, where the dashed lines denote the electrons moving out relative to the atomic electrons' superpositions in the bonding process. The figures indicate that electrons accumulate between the Ti and O atoms, implying strong covalent characteristics.

In order to give a quantitative analysis of the charge transfer according to the bonding process, we calculated the average atomic basin charge based on the AIM theory, and the results are listed in table 1. The patterns of the trajectories of $\nabla\rho(r)$ in the (100) and the (110) planes of cubic $BaTiO_3$ are also displayed in figure 4 (here parts of CP(3, 3) are omitted

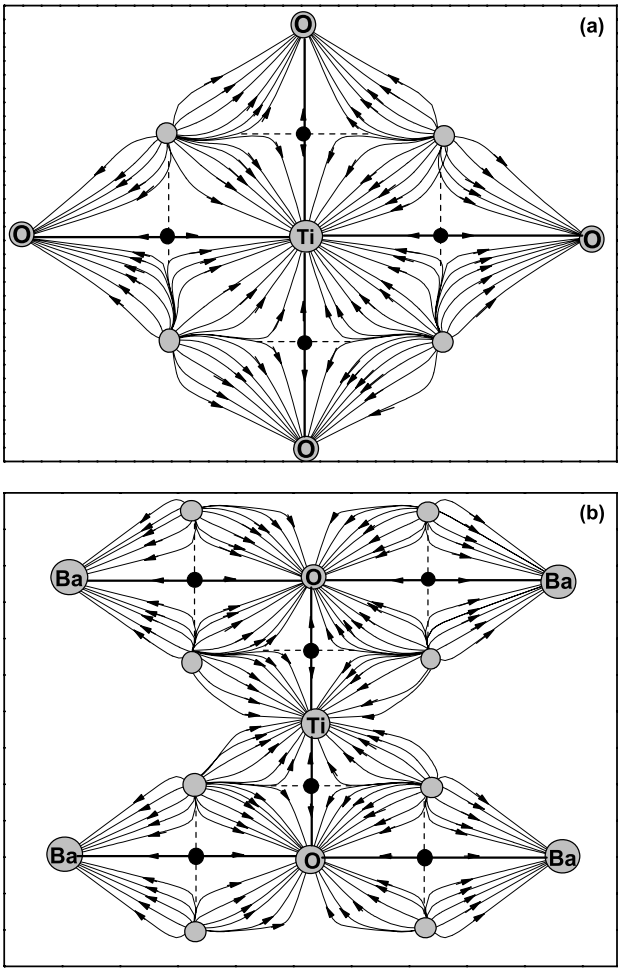

Figure 4. Trajectories of $\nabla\rho(r)$ in the (100) plane (a) and (110) plane (b) for the cubic phase. The arrows show the direction of some chosen trajectories. The dashed line is the intersection between the atomic basin surface for (100) and (110) planes. The bond CPs and cage CPs are labelled with black circles and grey circles respectively.

because of the symmetric distribution). Firstly, the results show a strong covalent characteristic between Ti and O. Secondly, there are some charges remaining in the Ba atomic basin, which means that the charges of the Ba ion are less than the nominal chemical charges (+2 for Ba). Namely, there are some covalent characteristics between Ba and the TiO_3 unit. The calculated results in the present study are in good agreement with those of previous works [37, 38]. The calculated basin charges show that the charges in the Ti and O1 atomic basin for the tetragonal phase are less than those of cubic phase. And the charges in the O2, O3 and Ba atomic basin for the tetragonal phase are larger than those of the cubic phase. The difference of the basin charges between the two phases mainly come from ferroelectric distortions which include a small macroscopic lattice strain and microscopic displacement of ions. The distortions change the p–d coupling strength between Ti and O, which induces a redistribution of the bonding charges. The details will be discussed below.

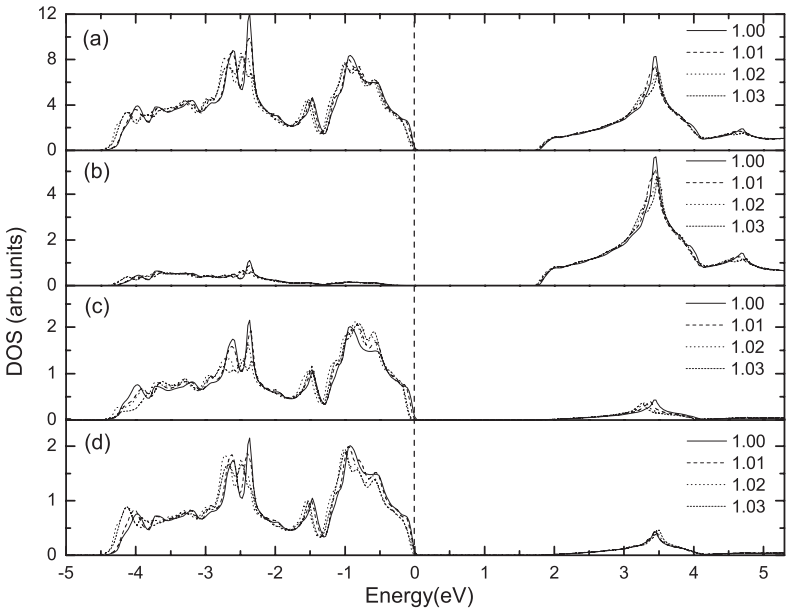

Figure 5. Total DOS and the PDOS of $BaTiO_3$ for four strains. (a) Total DOS, (b) PDOS of Ti 3d state, (c) PDOS of O1 2p state, (d) PDOS of O2, O3 2p states. Solid, dashed, dotted and short dashed lines denote the strain values 1, 1.01, 1.02 and 1.03, respectively.

Table 2. Average charge in atomic basin of Ba, Ti, O1, O2 and O3 according to the macroscopic strains ($c/a = 1$, 1.01, 1.02 and 1.03).

c/a	Ba	Ti	O1	O2	O3
1.00	1.547	2.225	−1.255	−1.255	−1.255
1.01	1.550	2.223	−1.259	−1.253	−1.253
1.02	1.550	2.222	−1.264	−1.250	−1.250
1.03	1.550	2.222	−1.268	−1.248	−1.248

3.2. Effects of lattice strain

Experimentally, there is a $c/a = 1.01$ strain in the tetragonal phase of $BaTiO_3$. In order to understand the strain on the bonding mechanism, we have chosen four different c/a ratios, $c/a = 1$, 1.01, 1.02 and 1.03, to investigate the evolution of the bonding mechanism; $c/a = 1$ corresponds to the cubic phase. In order to simplify the calculations, ion displacement is not considered here. Figure 5 shows the results of the DOS and the partial DOS (PDOS) for different strains. The results indicate that the lattice strain broaden the width of the DOS at the valence band region compared with that of the cubic phase. As the strain is increased, the total DOS becomes increasingly smooth. Meanwhile, the lattice strain leads to charge transfer between the atomic basins. The average charges according to different strains in Ba, Ti, and O atomic basin are listed in table 2. The average atomic basin charges of O1 increase as the strain increases. It is well known, that the c/a lattice strain at fixed volume increases the Ti–O1 distance and decreases the Ti–O2(O3) distance in the TiO_3 unit, which facilitates the (001) ferroelectric distortion. The difference of the average atomic charge between O1 and O2(O3) indicates that the c/a distortions cause the bonding strength between Ti and O in the

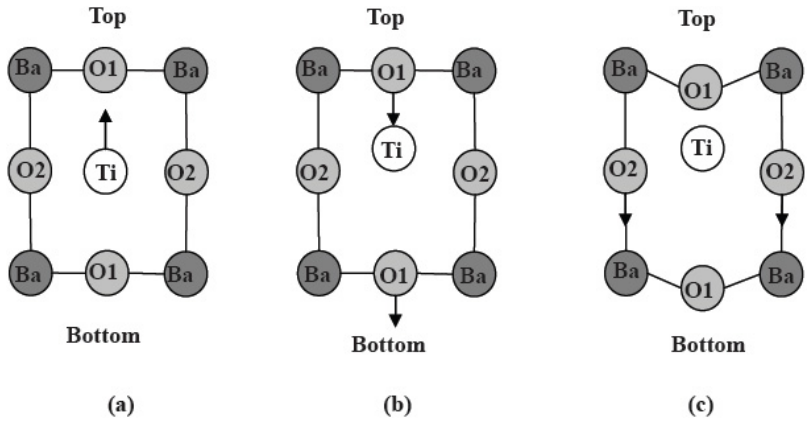

Figure 6. Three steps of the ion displacements. (a) Ti displaced along the [001] direction, (b) O1 displaced along the [00$\bar{1}$] direction, (c) O2(O3) displaced along the [00$\bar{1}$] direction.

TiO_3 octahedral unit to become unbalanced. The unbalanced bonding situation induces the displacements of Ti and O ions, which further induce the polarization. The results also indicate that, as the lattice strain becomes larger, the atomic charge of O1 increases and that of O2, O3 decreases. As we know, the hybridization between Ti 3d and O 2p plays an important role in the TiO_3 octahedral bonding mechanism. So the charge transfer between the Ti and O can be decomposed into two parts. Firstly, the hybridization between O 2p and Ti 4s makes the bonding charge close to the O ion. The charge transfer is found to occur from the Ti atomic basin to the basins of O. Secondly, the coupling between Ti 3d and O 2p states pulls the bonding charge back to the cation because of the localization of the d orbitals around Ti. Consequently, the atomic charge in O1, O2 and O3 tends to be larger (smaller) as the bond length becomes longer (shorter) along with the lattice strain. On the other hand, the charge in the Ba atomic basin increases according to the lattice strain, which means the ionicity between Ba and TiO_3 unit in the tetragonal phase is larger than that of the cubic one.

3.3. Effects of ion displacements

Experimentally, the ions are located at $(a/2, a/2, c/2 + \Delta\mathrm{Ti})$, $(a/2, a/2, -\Delta\mathrm{O1})$, $(0, a/2, c/2 - \Delta\mathrm{O2})$, $(a/2, 0, c/2 - \Delta\mathrm{O3})$ and (0, 0, 0) for Ti, O1, O2, O3 and Ba ions, respectively, for the ferroelectric phase. ΔTi, ΔO1, ΔO2, and ΔO3 are the displacements for Ti, O1, O2 and O3 relative to the ideal tetragonal structure, respectively. According to the experimental results, ΔTi, ΔO1 and ΔO2(O3) are 0.055, 0.101, and 0.061 Å, respectively. In order to investigate the effects of ion displacements on the bonding mechanism, we decomposed the ion displacements into three steps, as shown in figure 6. Firstly, the Ti ion is displaced along the [001] direction from zero to 0.10 Å (ΔTi = 0, 0.055 and 0.10 Å, respectively), and ΔO1 = ΔO2 = ΔO3 = 0. Secondly, the O1 ion is displaced along the [00$\bar{1}$] direction from zero to 0.20 Å (ΔO1 = 0, 0.101 and 0.20 Å, respectively), and ΔO2 = ΔO3 = 0, ΔTi = 0.055 Å. Lastly, O2 and O3 ions are displaced along the [00$\bar{1}$] direction from zero to 0.15 Å (ΔO2 = ΔO3 = 0, 0.061 and 0.15 Å, respectively), and ΔTi = 0.055 Å, ΔO1 = 0.101 Å. In this way, we can describe the effects of the ion displacements on the bonding mechanisms clearly and separately.

The DOSs following the three different ion displacement steps were calculated; they are shown in figure 7. The displacement of Ti leads to a trivial down-shift of the valence band, as

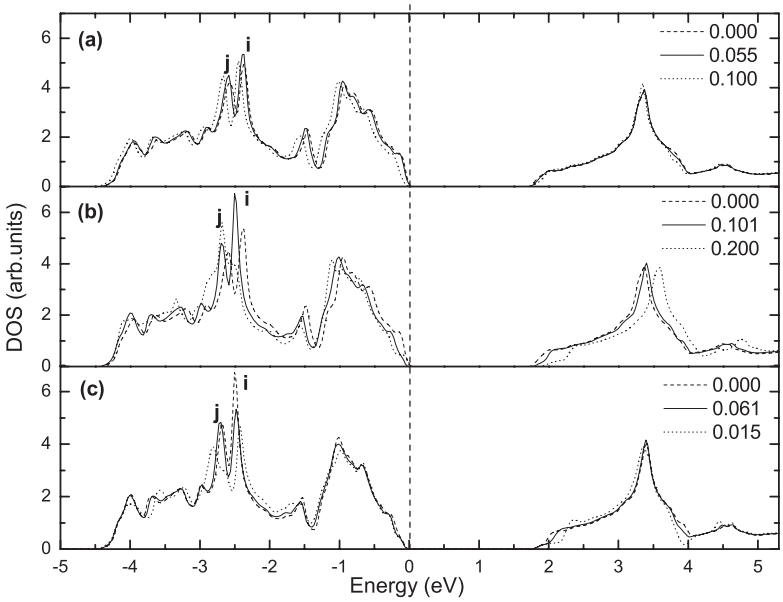

Figure 7. DOS of tetragonal structure $BaTiO_3$ with different ion displacements. (a) Ti displacements; (b) O1 displacements; (c) O2, O3 displacements.

shown in figure 7(a). The displacement of O1 gives rise to a large down-shift of the valence band and up-shift of the conduction band states, which enlarges the band gap. The band gap increases by about 0.11 eV as O1 is displaced to the site of the stable ferroelectric phase. The peaks of the DOS at the valence band region are also changed with the displacement of O1. Typically, on increasing of the displacement, peak *i* becomes weaker and peak *j* becomes sharper. Although the displacement of O2 and O3 does not give rise to a DOS energy shift as large as that of the O1 ion, both *i* and *j* peaks are also now obviously weaker. The valence and conduction band also shift inversely and the band gap is enlarged by about 0.03 eV. In summary, the calculated results indicate that the ferroelectric distortions increase the band gap by about 0.18 eV.

The p–d hybridization is sensitive to the shift of the bond length, and the change of the hybridized strength determines the charges in the atomic basin, as mentioned above. The ion displacements produce the bond length shift and further induce the change of the charge transfer among ions. The average atomic basin charges based on AIM theory show that the charges in the Ba atomic basin (1.550 electrons) are almost independent of the displacements of the ions. As for the TiO_3 unit, the charge transfer between Ti and O can be summarized as follows: (i) there are more than 0.02 electrons that transfer into the Ti and O1 atomic basins due to the opposite displacement between Ti and O1. The displacement of O2 and O3 leads to a trivial decrease of the charges in the Ti and O1 atomic basins. (ii) The charges in O2 and O3 atomic basins increase (0.01 electrons) as the Ti and O1 ions are displaced, and trivially decreased as O2 and O3 ions are displaced. Cohen [12] has pointed out that the long-range Coulomb forces favour the ferroelectric state and the short-range interatomic repulsive forces favour the paraelectric phase. Based on Cohen's statements, the decrease of the charge transfer from the Ti atomic basin into the O atomic basin weaken the short-range repulsive forces and favour the stabilization of the ferroelectric tetragonal phase. Therefore, opposite displacement between Ti and O is very important for stabilizing the tetragonal structure.

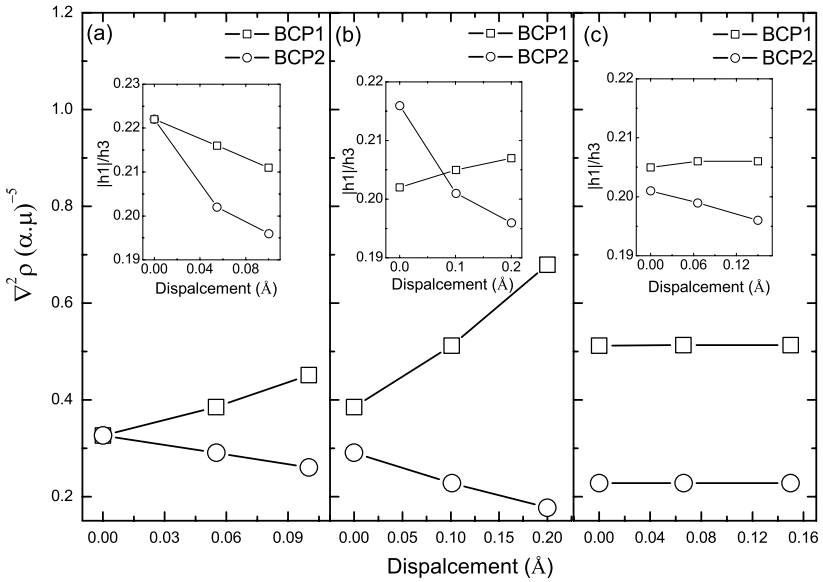

Figure 8. Laplacian $\nabla^2\rho$ of Ti–O1 bond CP according to different ion displacements. (a) Ti displacements; (b) O1 displacements; (c) O2(O3) displacements. The insets are the ratios $|h1|/h3$ according to different ions displacements.

According to the definition, a CP is a point where the gradient of a charge density vanishes. Calculating the Hessian of the density, we can characterize each critical point by the principal curvatures of the charge density (eigenvalues of the Hessian). As mentioned above, the CP $(3, -1)$ is called a bond CP that corresponds to a saddle point of ρ. Such a point is found between every pair of neighbouring nuclei, as shown in figure 4. Bader has pointed out that the presence of a bond path is a necessary condition for two atoms to be bonded to one another [27]. For a bond CP, the two curvatures calculated in the directions perpendicular to the bond are equal ($h1$ and $h2$). The ratio of principal curvatures $|h1|/h3$ together with the Laplacian provides the information for a classification of chemical bonding. A small value $|h1|/h3 \ll 1$ is typical for closed-shell (ionic) interactions, while for covalent bonding the ratio increases with the increase of bond strength. Accordingly, the Laplacian is positive and large for ionic bonding, but small or negative for covalent bonds. The dependence of the Laplacian and the curvature ratio $|h1|/h3$ on the different ion displacements for the most important bond CP $(3, -1)$ (BCP) between Ti and the top O1 (BCP1) and between Ti and the bottom O1 (BCP2) are shown in figure 8. The results indicate that the Laplacian of BCP1 increases and the Laplacian of BCP2 decreases as Ti and O1 ions are oppositely displaced. This means that the opposite displacements between Ti and O1 increase (reduce) the ionic nature of the bond between Ti and top (bottom) O1. At the same time, the bond strength for both Ti–O1 bonds decrease as the ion displacement. The Laplacian and the curvature ratio $|h1|/h3$ for two kinds of BCP almost remain invariable when the O2 and O3 ions are displaced.

In summary, our quantitatively calculated results are very consistent with the results of previous works [39]. But, some important points should be mentioned here. Firstly, the influences of the lattice strain and ion displacements on the bonding nature are not restricted to Ti and O atoms but also involve Ba. In particular, the ionicity between Ba and the TiO_3 unit increases corresponding to the lattice strain. Moreover, the results shown in present paper indicate that there is more covalent character between Ba and the TiO_3 unit than in those

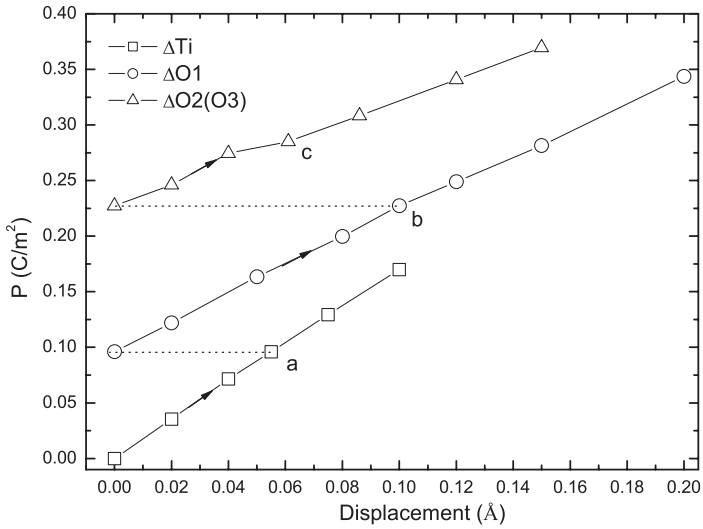

Figure 9. Spontaneous polarization according to the displacement of ions (Ti, O1 and O2(O3)). Square, circle and star denote the displacement of Ti, O1 and O2(O3), respectively. The direction of the arrow shows the trend of polarization corresponding to ion displacements. Characters a–c denote the polarization as the ion is displaced to the experimental siting at each step.

previous assumptions. Secondly, the lattice distortions reduce the bond strength between Ti and O. Finally, the charges in the TiO_3 unit are sensitive to lattice distortions, and the deflections of the atomic basin charges will lead to a spontaneous polarization along the direction of ion displacement; details will be discussed below.

3.4. Spontaneous polarization

Although we can predict that the ferroelectric distortions produce the deflection of the atomic basin charges and induce spontaneous polarization, we cannot describe the polarization accurately by the basin charges. According to the modern theory of polarization, the macroscopic polarization is best defined as a Berry phase of the electronic Bloch wavefunctions. The basin charges are derived from the charge density which comes from the square modulus of the occupied orbitals, so the any phase information is lost. Therefore, in order to give the dependence of the polarization **P** on the ion displacements, we have applied the Berry phase (or 'modern') theory of polarization [32–34]. The calculations are restricted to ion displacements along the c axis in a fixed tetragonal structure with $c/a = 1.01$. The centrosymmetric structure without ion displacements was chosen as the reference structure in our calculations, and its polarization is zero. In this approach, it is assumed that the transformation from the ideal centrosymmetric structure (tetragonal structure without ion displacements) to the polar structure (tetragonal structure with ion displacements) is a continuous adiabatic path. The total polarization **P** for a polar structure can be calculated as the sum of the ionic and electronic contributions. The electronic contribution to the polarization is calculated as a geometric phase, formally equivalent to the sum of Wannier centres of the occupied band. Detailed discussions of the modern theory of polarization can be found in [32].

In this way, we can investigate the contributions of the different ion (Ti, O1 and O2(O3)) displacements to the spontaneous polarization, and the calculated results are shown in figure 9. The calculated results show that the polarization **P** increases linearly according

to the displacements of all the three types of ions. The polarization **P** increases from 0.00 to 0.071 C m^{-2} when Ti is displaced from 0.00 to 0.10 Å. While the Ti ion is situated at the experimental lattice site, the polarization is 0.037 C m^{-2}. The polarization **P** increases from 0.037 C m^{-2} to 0.344 C m^{-2} as the O1 ion is displaced from 0.0 to 0.20 Å (while the Ti remains at the experimental site). While Ti and O1 are situated at the experimental lattice site, the polarization **P** increases from 0.227 to 0.370 C m^{-2} as O2(O3) ions are displaced from 0.00 to 0.15 Å. The lowercase letter *c* denotes the polarization as all the ions are situated at equilibrium sites, and the polarization is 0.282 C m^{-2} (as shown in figure 9) which is in good agreement with the experimental value (0.26–0.27 C m^{-2}) [40, 41]. Part of the error could be attributed to the fact that our calculated value is an upper limit, related to an idealized perfect crystal. A real sample always presents defects that tend to lower the measured polarization.

As we know, the macroscopic electric polarization relies on the dynamic process of charge redistribution, which is strongly related to the bonding mechanism of the system. Figure 9 shows that relative displacements of Ti–O lead to an increase of the polarization. Such an increase in the polarization can be readily understood in terms of the covalent nature involved in the orbital hybridizations between Ti–O, as mentioned above. As the ions are displaced, the average strength of the hybridization between Ti d and O p states is weakened, which softens the Ti–O repulsion and allows the ferroelectric instability. Therefore, a strong dynamic charge transfer takes place as the bond length is varied, which strengthens the long-range Coulomb interactions and favours the ferroelectric distortions.

4. Conclusions

The effects of ion displacements and lattice strain on the bonding mechanism of ferroelectrics perovskite material $BaTiO_3$ have been studied by using the FP-LAPW method in combination with the AIM theory. The density of states, the charge density and the charge transfer between atomic basins have been calculated for both cubic and tetragonal phase of $BaTiO_3$. The results indicate that the contributions to the valence states not only come from O and Ti atoms but also from the Ba atom. Charge density and Bader's topological analysis show strong deflections of p–d hybridization accompanying the ferroelectric displacements. The results also show a covalent nature of Ti–O bond and an incomplete ionic characteristic between Ba and the TiO_3 unit. The analysis of the effects of ion displacement on the bonding mechanism indicates that the charge transfer between atomic basins contributes to the stabilization of the tetragonal phase and produces a polarization along the direction of ion displacement. At the same time, the Ti–O bond strength will be reduced according to the relative displacements of Ti and O. The spontaneous polarization (0.282 C m^{-2}) calculated by the Berry phase theory of polarization is very consistent with experimental data. The nearly linear evolutions of the spontaneous polarization according to different ion displacements are also found in present paper.

Acknowledgments

This work is supported in part by the Scientific Research Fund of Hunan Provincial Education Department (06B092), Chinese National Key Basic Research Special Fund, Key fund of Chinese National Natural Science Foundation (10234040), the National Natural Science Foundation of China (60476040, 60576068, 10525211, 50561060), Grand Foundation of Shanghai Science and Technology (05DJ14003), and computational support from Shanghai Supercomputer Center.

References

[1] Cohen R E and Krakauer H 1990 *Phys. Rev.* B **42** 6416–23
[2] King-Smith R D and Vanderbih D 1994 *Phys. Rev.* B **49** 5828–44
[3] Resta R, Posternak M and Baldereschi A 1993 *Phys. Rev. Lett.* **70** 7
[4] Pertsev N A, Zembilgotov A G and Tagantsev A K 1998 *Phys. Rev. Lett.* **80** 1988
[5] Bungaro C and Rabe K M 2004 *Phys. Rev.* B **69** 184101
[6] Antons A, Neaton J B, Rabe K M and Vanderbilt D 2005 *Phys. Rev.* B **71** 024102
[7] Diguez O, Rabe K M and Vanderbilt D 2005 *Phys. Rev.* B **72** 144101
[8] Wessels B W 1995 *Annu. Rev. Mater. Sci.* **25** 525
[9] Millis A J 1998 *Nature* **392** 147
[10] Xue W D *et al* 2005 *Acta. Phys. Sin.* **54** 2 (in Chinese)
[11] Pauling L 1960 *The Nature of the Chemical Bond* (Ithaca, NY: Cornell University Press)
[12] Cohen R E 1992 *Nature* **358** 136
[13] Saha S and Sinha T P 2000 *Phys. Rev.* B **62** 13
[14] Miura K and Tanaka M 1998 *Japan. J. Appl. Phys.* 1 **37** 6451
[15] Miura K and Tanaka M 1998 *Japan. J. Appl. Phys.* 1 **37** 6460
[16] Bader R F W 1990 *Atoms in Molecules A Quantum Theory* (London: Oxford University Press)
[17] Yamaguchi M, Inoue K, Yagi T and Akishige Y 1995 *Phys. Rev. Lett.* **74** 2126
[18] Blaha P, Schwarz K, Madsen G, Kvasnicka D and Luitz J 2001 *WIEN2k An Augmented Plane Wave + Local Orbitals Program for Calculating Crystal Properties* Karlheinz Schwarz, Techn. University Wien, Austria (ISBN 3-9501031-1-2)
[19] Hohenberg P and Kohn W 1964 *Phys. Rev.* **136** B864
Kohn W and Sham L J 1965 *Phys. Rev.* **140** A1133
[20] Perdew J P, Burke K and Ernzerhof M 1996 *Phys. Rev. Lett.* **77** 3865
[21] Singh S N and Krakauer H 1991 *Phys. Rev.* B **43** 6411
[22] Bader R F W and Hssen H 1984 *J. Chem. Phys.* **80** 1943
[23] Bader R F W 1975 *MTP Int. Rev. Sci.: Phys. Chem. Ser. Two* **1** 43
[24] Runtz G R, Bader R F W and Messer R R 1977 *Can. J. Chem.* **55** 3040
[25] Bader R F W, Anderson S G and Duke A J 1979 *J. Am. Chem. Soc.* **101** 1389
[26] Bader R F W, Nguyen-Dang T T and Tal Y 1981 *Rep. Prog. Phys.* **44** 893
[27] Bader R F W 1998 *J. Phys. Chem.* A **102** 7314
[28] Bader R F W 1991 *Chem. Rev.* **91** 893
[29] Bader R F W 1985 *Acc. Chem. Res.* **18** 9
[30] Katan C, Rabiller P, Lecomte C, Guezo M, Oison V and Souhassou M 2003 *J. Appl. Crystallogr.* **36** 65
[31] Madsen G K H, Gatti C, Iversen B B, Damjanovic Lj, Stucky G D and Srdanov V I 1999 *Phys. Rev.* B **59** 12359
[32] King-Smith R D and Vanderbih D 1993 *Phys. Rev.* B **47** 1651
[33] Vanderbih D and King-Smith R D 1994 *Phys. Rev.* B **48** 4442
[34] Resta R 1994 *Rev. Mod. Phys.* **66** 899
[35] Kresse G and Furthmůller J 1996 *Comput. Mater. Sci.* **6** 15
[36] Kresse G and Joubert D 1999 *Phys. Rev.* B **59** 1758
[37] Turik A V and Khasabov A G 1988 *Ferroelectrics* **83** 165
[38] Xu Y N, Hong J, Zhong X-F and Ching W Y 1994 *Ferroelectrics* **153** 19
[39] Filippetti A and Hill N A 2002 *Phys. Rev.* B **65** 195120
[40] Wieder H H 1955 *Phys. Rev.* **99** 1161
[41] Merz W J 1952 *Phys. Rev.* **88** 421